A Time-Weighted Dynamic Time Warping method for land use and land cover mapping

Victor Maus, Gilberto Câmara, Ricardo Cartaxo, Alber Sanchez, Fernando M. Ramos, Gilberto Q. Ribeiro

***Abstract*—A major recent trend in remote sensing research is the analysis of satellite image time series for land use and land cover monitoring and mapping. In this paper, we describe the Time-Weighted Dynamic Time Warping algorithm, which improves on previously proposed methods for land cover and land use classification. The method is based on the dynamic time warping method that measures similarity between two temporal sequences. We modified this method to account for seasonality of land cover types. The resulting algorithm is flexible to account for different cropland systems, tropical forests, and pasture using few training samples. The algorithm had better results than other Dynamic Time Warping variations for land classification. The method is suitable to make land use and land cover maps and has potential for large-scale analysis at country or continental scale, using global data sets such as the EVI time series from the MODIS sensor.**

Keywords*—Time series analysis, MODIS time series, Land use changes, Crop monitoring.

I. Introduction

Since remote sensing satellites revisit the same place repeatedly, we can adjust their images so measures of the same place in different times are comparable. From a data analysis perspective, researchers then have access to space-time data sets. This has lead to growing research on satellite image time series analysis. Algorithms for analysing image time series include methods for time series reconstruction [1], for detecting trend and seasonal changes [2]–[4], for extracting seasonality information [5], land cover mapping [6], detecting forest disturbance and recovery [7]–[9], crop classification [10]–[12], planted forest mapping [13], and crop expansion and intensification [14], [15].

This paper describes a new image time series analysis algorithm which improves on previously proposed methods for land cover and land use classification. Our method uses a time-weighted version of the Dynamic Time Warping (DTW) algorithm. DTW works by comparing a temporal signature of a known event (e.g. a person's speech) to an unknown time series (e.g. a speech record of unknown origin) [16]–[20]. The algorithm compares two time series and finds their optimal alignment, providing a dissimilarity measure as a result [19]. DTW provides a robust distance measure for comparing time series, even irregularly sampled or if they are out of phase in the time axis [21].

V. Maus, G. Câmara, R. Cartaxo, A. Sanchez, F.M. Ramos and G.Q. Ribeiro are with the National Institute for Space Research, Avenida dos Astronautas 1758, 12227010, São José dos Campos, Brazil (e-mail: victor.maus@inpe.br).

V. Maus and G. Câmara are also with the Institute for Geoinformatics, University of Münster, Heisenbergstrae 2, 48149, Münster, Germany.

The original DTW algorithm is not well suited for time series analysis of land use and land cover data. It disregards the temporal range when finding the best alignment between two time series [19], [22]. However, when dealing with land change, we cannot ignore time completely. Each agricultural crop has a distinct phenological cycle that is relevant for space-time classification [23], [24]. Consider, for example, the difference between the phenological cycles for crops, such as, soybean and corn ranging from 90 to 120 days and sugarcane from 360 to 520 days. To distinguish between these cycles, it is useful to include a temporal weighting function in the DTW method.

Recent papers by [12] and [25] have used DTW for satellite image time series classification. The method proposed in these papers sets a maximum time delay to avoid inconsistent temporal distortions based on the date of the satellite images. The time series is split in one year segments to match the agricultural phenological cycle in Europe. However, this temporal segmentation reduces the power of the DTW classifier. Crops with phenological cycles longer than one year or taking place in different seasons may not be detected. To avoid this problem, we introduce a time-weighted extension to the DTW algorithm, which classifies temporal segments of a remote sensing time series without splitting it into fixed parts. This method is flexible to account for multiyear crops, single cropping and, double cropping. It is also robust to account for other land cover types such as forest and pasture and works with a small amount of training samples.

This paper describes the time-weighted DTW algorithm (TWDTW) for land use and land cover classification and compares the TWDTW accuracy with the original DTW algorithm without time constraints and with the time delay DTW proposed by [12]. We show a case study area in the Brazilian Amazon with high land changes dynamics and compare the results with other land use and land cover products.

II. Methods

Remote sensing satellites cycle the Earth at regular intervals, and thus their data are mappable to a three-dimensional array in space-time Fig. (1a). Each pixel location (x, y) in consecutive times, $t_1, ..., t_m$, makes up a satellite image time series (SITS), from that we can extract land use and land cover information, such as the SITS in Fig. (1b). In the example, during the first two years the area was covered by forest, then it was deforested in 2002. The area was then used for cattle raising (pasture) for three years. After that, it was used for crop production for three years from 2006 to 2008.

Let $\mathbf{V}_{x,y} = (v_1, v_2, ..., v_m)$ be a time series of a pixel location (x, y) in consecutive times, $t_1, ..., t_m$, where v is

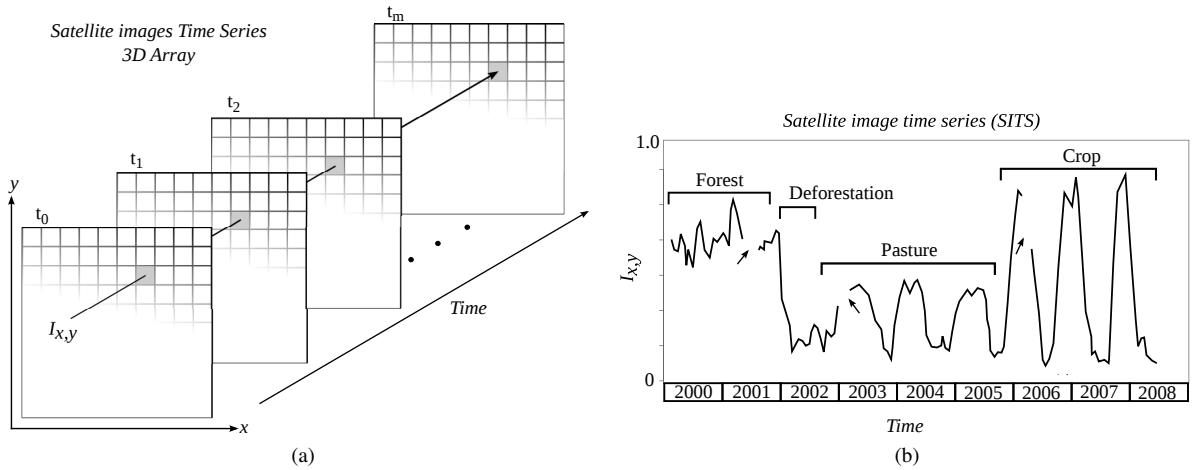

Fig. 1: (a) A 3-dimensional array of satellite images, (b) a vegetation index time series I at the pixel location (x, y). The arrows indicate data gaps.

the value of the sensor measure at time t. For the satellite's coverage, we get a set of time series $\mathcal{S} = \{\mathbf{V}_1, \mathbf{V}_2, ..., \mathbf{V}_s\}$. We want to classify time intervals of this set into one of the possible land use and land cover classes. Each temporal interval, ideally, corresponds to a stable period of land cover and land use, that we want to associate with one of our land classes. For example, suppose a ten year period where in the first five years the area was covered by forest. The area was then used for cattle raising (pasture) for two years. After that, it was used for soybean production for three years. We want to associate each of these intervals with one of our land classes.

Optical remotely sensed data are affected by cloud cover that introduces a large amount of noise in STIS, as shown in Fig. (1b). Inter-annual climate variability also changes the phenological cycles of the vegetation, resulting in STIS whose periods and intensities do not match on an year to year basis [23]. To associate intervals of a SITS with land cover and land use classes, we need methods suitable for noisy and out-of-phase time series. We chose the Dynamic Time Warping (DTW) algorithm because it is suitable for this problem.

The papers by [12] and [25] applied the DTW algorithm to classify intervals of SITS, such as in Fig. (2a). In this case, two time series have approximately the same length and the first and last points in both time series must match. In practice, crop phenological cycles can vary in an year-to-year basis, depending on climate conditions and land management, for example shifting the greenup and dormancy stages of the vegetation [23], [24]. To avoid possible inconsistent matching of phenological cycles caused by splitting the time series we use an open boundary version of DTW, Fig. (2b). The open boundary method does not require two time series to be of the same length, and it is suitable to find all possible matches of one pattern within a long-term time series [26].

The open boundary DTW algorithm disregard the time dimension and can cause inconsistent phase alignments, e.g. an winter crop can match in the summer time with low DTW distance. Therefore, we introduce an extra cost that controls the time warping and makes the time series alignment dependent on the dates of the year. This is especially useful for detecting seasonal crops and for distinguishing pasture from agriculture.

Our classification method using open boundary DTW [26] requires matching subsequences of the time series associated with each pixel location to samples of the expected classes. For each class c, we take a set of time series samples $\mathcal{Q}_c = \{\mathbf{U}_1, \mathbf{U}_2, ..., \mathbf{U}_q\}$, where $\mathbf{U} = (u_1, ..., u_n)$ is a time series with $n \ll m$ (i.e. the pattern length is much shorter than the sensor time series $\mathbf{V}$). These samples are then used to classify the intervals of the time series $\mathbf{V} \in \mathcal{S}$.

The classification runs independently for each pixel location and has two steps. We start applying the DTW algorithm for each pattern in $\mathcal{Q}$ and each time series $\mathbf{V} \in \mathcal{S}$. This step provides information about the matches of the patterns within the time series. In the second step we use the DTW matches to build the sequence of land use and land cover maps.

A. Step 1: DTW Alignment

The DTW alignment starts by computing a n-by-m matrix Ψ, whose elements $\psi_{i,j}$ are the absolute difference between $u_i \in \mathbf{U}\ \forall\ i = 1, ..., n$ and $v_j \in \mathbf{V}\ \forall\ j = 1, ..., m$. From Ψ we compute an accumulated cost matrix $\mathbf{D}$ by a recursive sum of the minimal distances, such that

$$d_{i,j} = \psi_{i,j} + min\{d_{i-1,j}, d_{i-1,j-1}, d_{i,j-1}\}, \qquad (1)$$

that is subject to the following boundary conditions:

$$d_{i,j} = \begin{cases} \psi_{i,j} & i = 1,\ j = 1 \\ \sum_{k=1}^{i} \psi_{k,j} & 1 < i \leq n,\ j = 1 \\ \sum_{k=1}^{j} \psi_{i,k} & i = 1,\ 1 < j \leq m \end{cases} \qquad (2)$$

The Fig. (3) shows an example of the accumulated cost matrix $\mathbf{D}$. Intuitively, the DTW alignment runs along the "valleys" of low cost within the accumulated cost matrix $\mathbf{D}$, that has as many "valleys" as the number of matches between

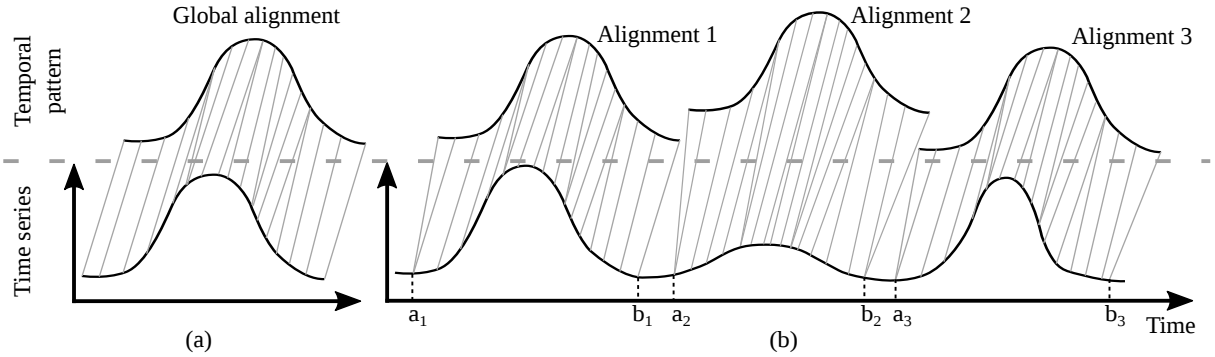

Fig. 2: (a) DTW Alignment between two time series with approximately same length, (b) DTW alignments between a pattern whose length is much shorter than the time series. The indexes a are starting points and b ending points of each interval in the long-term time series.

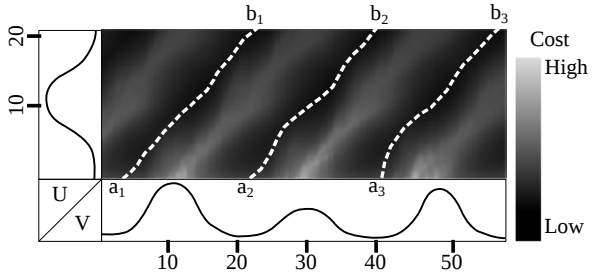

Fig. 3: Accumulated cost matrix D showing three possible alignment of the pattern $\mathbf{U}$ within the long-term time series $\mathbf{V}$. The indexes a are starting points and b ending points of each DTW alignment in $\mathbf{V}$.

$\mathbf{U}$ and $\mathbf{V}$. The kth low cost path in $\mathbf{D}$ produces an alignment between the pattern and a subsequence $\mathbf{V}|_{a_k}^{b_k}$ with associated DTW distance δ_k, where a_k is the starting point and b_k the ending point of the subsequence k [26], as shown in Fig. (3).

Each minimum point in the last line of the accumulated cost matrix, i.e. $d_{n,j}\ \forall\ j = 1, ..., m$, produces an alignment, with b_k and the δ_k given by,

$$b_k = argmin_k(d_{n,j}), \quad k = 1, ..., K \tag{3}$$

$$\delta_k = d_{n,b_k} \tag{4}$$

where K is the number of minimum points in last line of the accumulated cost matrix.

A reverse algorithm, Eq. (5), maps the warping path $\mathbf{P}_k = (p_1, ..., p_L)$ along the kth low cost "valley" in $\mathbf{D}$. The algorithm starts in $p_{l=L} = (i = n, j = b_k)$ and ends when $i = 1$, i.e. $p_{l=1} = (i = 1, j = a_k)$, where L denotes the last point of the alignment. The warping path $\mathbf{P}_k$ contains the matching points between the time series. Note that the backward step in the Eq. (5) implies the monotonicity condition [17], [26], i.e. the alignment preserves the order of the time series.

$$p_{l-1} = \begin{cases} (i, a_k = j) & if \quad i = 1 \\ (i-1, j) & if \quad j = 1 \\ argmin(\begin{array}{ll} d_{i-1,j}, & \\ d_{i-1,j-1}, & \text{otherwise} \\ d_{i,j-1}) & \end{array} \end{cases} \tag{5}$$

The original DTW algorithm does not account for the phase difference between the time series [22]. However land use and land cover types have distinct phenological cycles that are relevant for space-time classification [23], [24]. Therefore, here we propose a Time-Weighted DTW (TWDTW) based on the date of each pixel in the satellite image. This time-weighted version of DTW adds a temporal cost ω to the cost matrix Ψ, whose elements become $\psi_{i,j} = |u_i - v_j| + \omega_{i,j}$. To compute the temporal cost we propose both a linear

$$\omega_{i,j} = g(t_i, t_j) \tag{6}$$

and a logistic model with midpoint β, and steepness α, such that

$$\omega_{i,j} = \frac{1}{1 + e^{-\alpha(g(t_i,t_j)-\beta)}}, \tag{7}$$

where $g(t_i, t_j)$ is the elapsed time in days between the dates t_i in the pattern and t_j in the time series. We ran many tests using different values of β and α. We then used the best global accuracy performance to set the parameters for the logistic time-weighted DTW.

B. Step 2: Map building

The DTW algorithm matches each pattern to the input time series independently from the others. Thus, each interval of the time series $\mathbf{V}$ can fit different patterns. To associate an interval of the time series $\mathbf{V}$ to a land cover and land use class, we choose the best fitting pattern, i.e. the pattern with the lowest DTW distance in the interval. After finding the best fit, we can produce maps that show a land cover and land use classification for a given period.

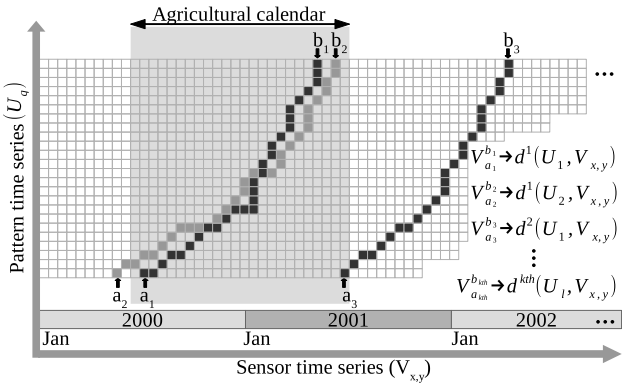

Fig. 4: Open boundary DTW alignment. Dark and light shades represent the alignments of the patterns U_1 and U_2, respectively. The indexes a_k and b_k represent the starting and ending points of the kth alignment in $\mathbf{V}$ associated with a DTW distance measure δ_k.

In our experiments, to compare our results with other land use/cover products, we produced maps matching the agricultural calendar from July to June (gray area in Fig. (4)). We find the pattern that has the lowest DTW distance to a subsequence $\mathbf{V}|_{a_k}^{b_k}$ partly contained in the crop calendar. The Fig. (4) shows the matching of two patterns, $\mathbf{U}_1$ and $\mathbf{U}_2$, that are partially in the same agricultural year from July 2000 to June 2001. In this case we pick the one with the lowest DTW distance, i.e. the most similar pattern for that period.

III. Experiments

Phenological cycles are strongly correlated with the seasons, which can not be completely ignored for the land use and land cover classification of STIS. Therefore, to assess the importance of the time dimension in the DTW analysis of SITS, we tested the performance of four different DTW methods: *i)* the original DTW algorithm without time constraints (i.e. $\omega = 0$), *ii)* DTW with maximum time delay as proposed by [12], *iii)* linear time-weighted DTW, and *iv)* logistic time-weighted DTW.

We used time series of Enhanced Vegetation Index (EVI) from July 2000 to June 2013 based on Moderate Resolution Imaging Spectroradiometer (MODIS) product MOD13-Q1 16 day 250 m. The MODIS EVI product is efficient to capture the vegetation signal. It has improved sensitivity in high biomass regions through a canopy background adjustment and a reduction in the atmosphere influences [27], [28].

The EVI time series is subject to atmospheric effects, such as cloud cover and path radiance from aerosols [29]. To reduce the spurious oscillation related to atmospheric effects, we apply a discrete wavelet decomposition [30] and then filter the time series by removing the highest wavelet frequency. The wavelet filter preserves the essential temporal variation and is more sensitive to vegetation seasonal changes than filters based on Fourier transform [31].

One scientific problem of particular importance to the authors is understanding changes in Brazilian Amazonia. The Brazilian Amazonian rain forest occupies an area of 4,100,000 km2 where 720,000 km2 have been deforested since the 1970s [32]. In the Copenhagen COP-15 Climate Conference in 2009, Brazil pledged to reduce deforestation in Amazonia by 80% relative to the average of the period 1996-2005. Brazil is making good this pledge, as deforestation in Amazonia fell from 27,700 km2 in 2004 to 4,900 in 2012, decreasing by 83%. Considering the significant impact of land changes in Amazonia on global biodiversity, emissions, and ecological services, it is important to understand the driving forces that cause forest removal [33]. INPE (Brazil's National Institute for Space Research) and EMBRAPA (Brazils Agricultural Research Agency) published recently a study that accounts for the land use of the deforested areas in Amazonia up to 2008 [34]. The results show that about 63% of the forest cuts are now used for cattle raising, including clean and degraded pasture. Cattle ranches in Amazonia use extensive practices, with less than 1 head of cattle per hectare. Cash crop agriculture accounts for only 4% of the deforestation. Moreover, more than 20% of the area has been abandoned and is now regrowing as secondary vegetation. To achieve further gains in reducing deforestation and biodiversity loss, we need to understand the different land use trajectories, including the deforestation dynamics, land use intensification, and land abandonment pathways.

We ran a case study in an area in Amazonia, Brazil, with strong deforestation and cropland expansion in the last decade. We selected the Porto dos Gaúchos municipality, that covers approximately 7,000 km^2 and is located in the state of Mato Grosso, Brazil, inside of the Amazon Biome. In 2013 its total deforested area was 3023.6 km^2, that is 42.9% of the original forest cover [32]. The cropland area grew from 59.8 km^2 in 2000 to 580.8 km^2 in 2013 [35]. We chose the most important classes for that area: forest, secondary vegetation, pasture, single cropping, and double cropping. These classes are the most relevant ones for our study on trajectories of change in Amazonia.

Our classification method requires a set of temporal patterns of the chosen land use/cover classes. Each pattern is the averaged EVI signal for a land cover class according to the agricultural calendar from July to June. We defined the temporal patterns of forest, pasture, single cropping, and double cropping based on the paper by [36], that presented typical temporal patterns of EVI for different crops and natural vegetation for the same region of our case study. Each class has one or two patterns that are showed in Fig. (5).

Since the EVI profile of "forest" and "secondary vegetation" is similar, after we find the best pattern for each map we split our "forest" class into "forest" and "secondary vegetation". This requires a land cover transition rule to split the "forest" class. Areas matching a forest pattern were classified as forest only if they were also classified as forest in previous years. Otherwise, we classified them as secondary vegetation. For the first year of the time series the areas matching a forest pattern are classified as forest, and therefore there is no secondary vegetation in the first year of our classification.

To assess our classification algorithm we used 40 random selected spatial location from 2001 to 2014 that sums up to 489

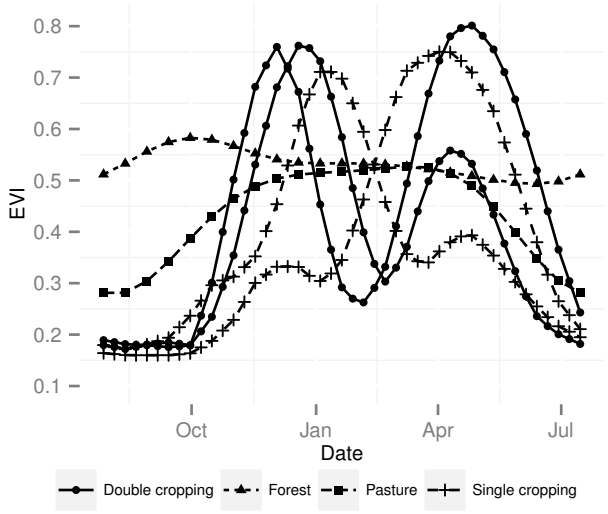

Fig. 5: Temporal patterns of EVI MODIS 16 days. Adapted from [36].

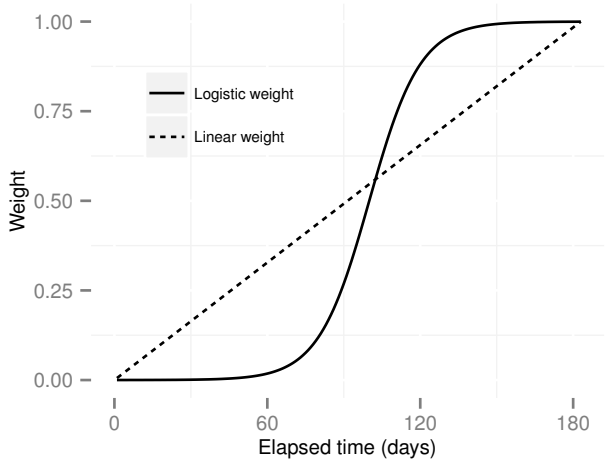

Fig. 6: Linear and logistic time-weight. The logistic weight has midpoint $\beta = 100\,days$ and steepness $\alpha = 0.1$.

TABLE I: Equivalent classes for comparison between the TWDTW classification and MODIS land cover collection 5, Plant Functional Type (PFT).

Aggregated	MODIS PFT	TWDTW
Forest	Evergreen Needleleaf trees, Evergreen Broadleaf trees, and Deciduous Broadleaf trees	Forest, and Secondary Vegetation
Pastureland	Shrub and Grass	Pasture
Cropland	Cereal crops, and Broad-leaf crops	Single cropping and Double cropping

samples. The samples were classified by visual interpretation of Landsat images using the Google Earth Engine [37]. To separate our classes we used a set of images corresponding to the agricultural year from July to June. For each year we used at least 4 images showing different phenological stages of the vegetation that allow us to distinguish: forest, pasture, single cropping, and double cropping.

We compared the accuracy of our classification and the MODIS land cover collection 5, Plant Functional Type (PFT) 500 m [38] based on our validation points. In order to compare our results with MODIS PFT we used the equivalent classes in Table I. Originally, the study area was covered by forest, and therefore, the other land cover types that appear later result from human activities. We aggregated the MODIS categories of trees to a class called forest. We also assume that MODIS shrub and grass classes are used as pastureland for cattle raising, and the categories of cereal crops and broad-leaf crops are aggregated to a class called cropland. Other MODIS classes are less than 0.008% of the pixels in this area, and thus they were not considered in this paper.

We also compared our forest area with estimations by the Amazon Monitoring Program PRODES [32], and the cropland area with the Brazilian national cropland surveys [35], which is the only existing source of annual information on land use. The cropland survey estimates come from public and private agents involved in the crop production and trade.

IV. Results

The logistic time-weighted DTW had the best performance for $\alpha = 0.1$ and $\beta = 100\,days$ (global accuracy 87.32%), meaning a low penalty for time warps smaller then $60\,days$ and significant costs for bigger time warps Fig. (6). In the algorithm proposed by [12] we tested maximum time delays ranging from 30 to $130\,days$, and found the best performance when the delay was set to $100\,days$ with global accuracy 84.66%. The linear Time-Weighted DTW had global accuracy 81.6% and the DTW without time restrictions only 70.14%.

The Table II shows the accuracy assessment of the four DTW approaches based on 489 reference samples classified from the Landsat images. In general, the logistic TWDTW had higher accuracy than the other approaches. Although the logistic TWDTW had lower *user accuracy* than the linear TWDTW for double cropping and forest, its *producer accuracy* was higher than the linear TWDTW for these classes (cf. Table II). This means that the logistic TWDTW classified more ground truth pixels as such, but with a slightly lower confidence than the linear TWDTW for pixels classified as double cropping and forest. The logistic TWDTW had the same value of sensitivity for double cropping as the maximum delay DTW (i.e. *producer accuracy* 90.43%), but with larger confidence for this class, *user accuracy* 92.04% in comparison to 88.89%.

The confusion matrices of the four DTW approaches are showed in Table III. The linear TWDTW classified 24 pixels of double cropping and 34 pixels of pasture as single cropping, and therefore, its confidence for single cropping was only 60.27% (cf. Table II). The logistic TWDW classified 10 pixels of double cropping and 18 pixels of pasture as single cropping,

TABLE II: Accuracy assessment for each class based on 489 reference samples classified from the Landsat images.

Method	Double cropping		Forest		Pasture		Single cropping	
	User (%)	Producer (%)	User (%)	Producer (%)	User (%)	Producer (%)	User (%)	Producer (%)
DTW without time restrictions	74.65	46.09	88.51	72.64	79.53	80.47	50.00	77.78
DTW with maximum delay of $100\,days$	88.89	90.43	93.00	87.74	88.20	84.02	72.82	75.76
Linear TWDTW	96.70	76.52	96.81	85.85	83.54	78.11	60.27	88.89
Logistic TWDTW for $\alpha = 0.1$ and $\beta = 100\,days$	92.04	90.43	94.00	88.68	88.41	85.80	75.00	84.85

TABLE III: Confusion matrices based on 489 reference samples classified from the Landsat images.

	Reference (%)			
Predicted (%)	Double cropping	Forest	Pasture	Single cropping
DTW without time restrictions				
Double cropping	53	2	4	12
Forest	0	77	7	3
Pasture	5	25	136	5
Single cropping	57	1	19	77
Unclassified	0	1	3	2
DTW with maximum delay of $100\,days$				
Double cropping	104	1	1	11
Forest	0	93	7	0
Pasture	2	11	142	6
Single cropping	9	1	18	75
Unclassified	0	0	1	7
Linear TWDTW				
Double cropping	88	0	0	3
Forest	0	91	3	0
Pasture	3	15	132	8
Single cropping	24	0	34	88
Unclassified	0	0	0	0
Logistic TWDTW for $\alpha = 0.1$ and $\beta = 100\,days$				
Double cropping	104	0	0	9
Forest	0	94	6	0
Pasture	1	12	145	6
Single cropping	10	0	18	84
Unclassified	0	0	0	0

which means a higher confidence than the linear TWDTW classification for single cropping, 75.00%. These results of the logistic TWDW were similar to the results obtained using the maximum time delay DTW, which classified 9 pixels of double cropping and 18 pixels of pasture as single cropping. However, the logistic TWDTW had higher sensitivity than the maximum time delay DTW (84.85% in comparison to 75.76% cf. Table II), that classified 11 pixels as double cropping, 6 as pasture and unclassified other 7 pixels out of 99 pixels of single cropping.

For the aggregated classes in Table I the logistic TWDTW had global accuracy 91.21% that is higher than the global accuracy of MODIS land cover collection 5 PFT, 79.36%. The accuracy assessment of the logistic TWDTW and the MODIS land cover is showed in Table IV. The logistic TWDTW had higher user and producer accuracies than the MODIS classification for all classes. Although, MODIS had high user accuracy for forest (87.2%) and cropland (89.33%), its producer accuracy for these classes was low, 77.37% and 75.28%, respectively.

We also compared the classification results with the Brazilian national cropland surveys [35]. Fig. (7) shows the area of single cropping and double cropping estimated by using

TABLE IV: Assessment of MODIS collection 5 Plant Functional Type (PFT) and logistic TWDTW based on 489 reference samples classified from the Landsat images. The classes forest, pastureland, and cropland were aggregated according to Table I.

	User (%)		Producer (%)	
Class	MODIS	TWDTW	MODIS	TWDTW
Forest	87.23	94.00	77.36	88.68
Pastureland	67.71	88.41	85.53	85.80
Cropland	89.33	92.00	75.28	96.73

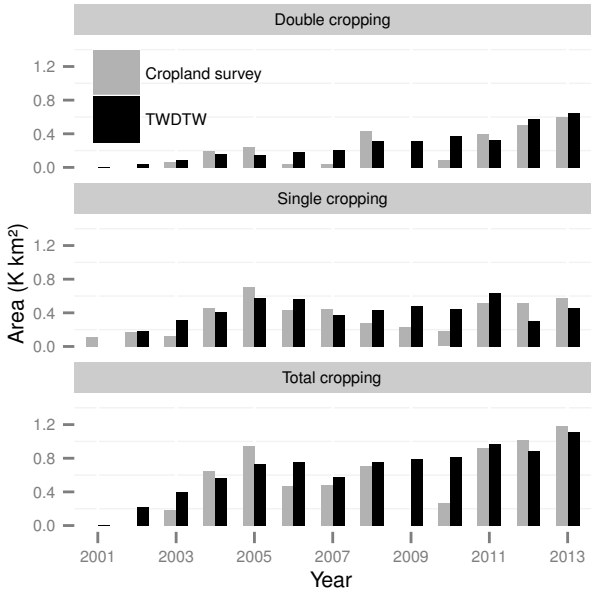

Fig. 7: Total area of double cropping and single cropping in Porto dos Gaúchos estimated by TWDTW and the Brazilian national cropland survey [35].

the logistic TWDTW algorithm and the Brazilian national cropland survey [35] for Porto dos Gaúchos. There is a general agreement between our results and the crop surveys, except in the years 2009 and 2010.

The total forest (pristine forest) and the secondary vegetation areas are presented in Fig. (8). The forest area estimated using the logistic TWDTW is in line with the area estimated by PRODES [32]. Most of the deforestation occurred before 2005, which was followed by an increase of the secondary vegetation

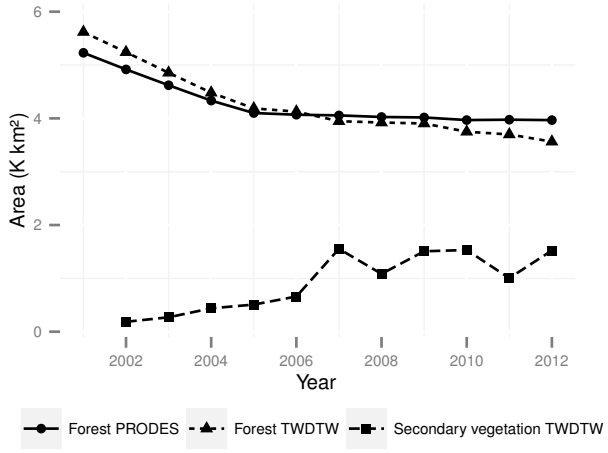

Fig. 8: Forest area estimated by the Amazon Monitoring Program PRODES [32] and using the logistic TWDTW based classification for Porto dos Gaúchos.

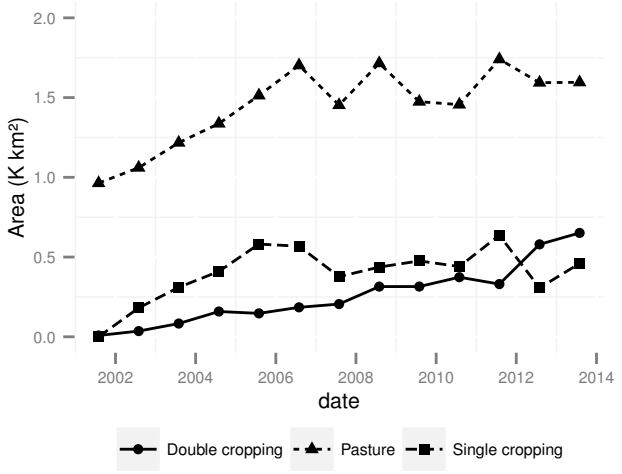

Fig. 9: Total area of pasture, single cropping, and double cropping from 2001 to 2013 estimated using logistic TWDTW for Porto dos Gaúchos.

area in 2007.

The total agricultural areas (pasture, single cropping, and double cropping) are showed in Fig. (9). In the time series, the pasture and single cropping areas were increasing until 2006, while the double cropping area has a growing trend during the whole period. In the last two years of the time series, the double cropping exceeded the single cropping area.

The Fig. (10) shows the spatial distribution of land use and land cover in Porto dos Gaúchos for each second agricultural year from 2001 to 2013. In the last decade, a cropland intensification has happened in the East part of Porto dos Gaúchos while pasture expansion has taken place in the West part.

V. Discussion

The results show that it pays to have a flexible approach to temporal restrictions when using DTW for land cover and land use classification. Completely disregarding the time dimension, as the original DTW method does, precludes an accurate land use and land cover classification. The maximum time delay, proposed by [12], is flexible for small time warps. However it forces the dynamic algorithm, Eq. (5), to map the warping path inside of a limiting time window that can preclude the classification of some areas (cf. unclassified samples in Table III). A large cost for small time warps, as the linear TWDTW method does, harms the classification and reduces its sensitivity. The linear TWDTW had low *producer's accuracy* respectively 78.11%, 76.52%, when classifying pasture and double cropping (cf. Table II). The phenological cycles in agricultural areas, i.e. pasture, double cropping, and single cropping, have great inter-annual variability depending on climate conditions and land management. The time constraints included in the DTW similarity measure should be flexible to handle with the small phase changes related to natural phenological variability. The logistic TWDTW had better results for these land use classes, because of its low penalty for small time warps and its significant costs for large time warps. Its better accuracy derives from its flexibility to find the best match between a pattern and an interval within a long-term time series.

The logistic TWDTW classification and other land use and land cover products are generally comparable. For example, our classification was in line with Brazilian national cropland surveys, except in the years 2009 and 2010, Fig. (7). In these years, it is likely that the cropland area has been underestimated in the survey because the large variations between 2008 and 2009 and between 2010 and 2011 are difficult to explain otherwise. Since the time-weighted DTW is a direct measure of the cropland area and its results are spatially distributed, we consider the TWDTW estimations more consistent than the cropland survey estimations.

The forest area estimated using the logistic TWDTW was similar to the forest area from the Amazon Monitoring Program (PRODES) Fig. (8). However, our algorithm gave higher estimates for the forest area until 2006 and lower estimates during the subsequent years. The higher forest area estimated by the logistic TWDTW compared to PRODES in the first years of the time series is likely related to their different scale of analysis. While we used MODIS images with 250 m spatial resolution the PRODES project uses 30 m Landsat images. Therefore PRODES is capable of detecting deforestation in small areas that may not be detected at the MODIS resolution.

In the second part of the graphic in Fig. (8), the lower forest area estimated by our method was caused by the transition rule used in our algorithm to separate the secondary vegetation from the forest. Applying this rule an area that changes from forest to any other land class cannot become forest again. For example, after a degradation event (e.g. by fire) the area is classified as secondary vegetation in our algorithm, cf. Fig. (11). Therefore, our estimation reduces from the forest area both deforested and degraded areas, whereas PRODES reduces

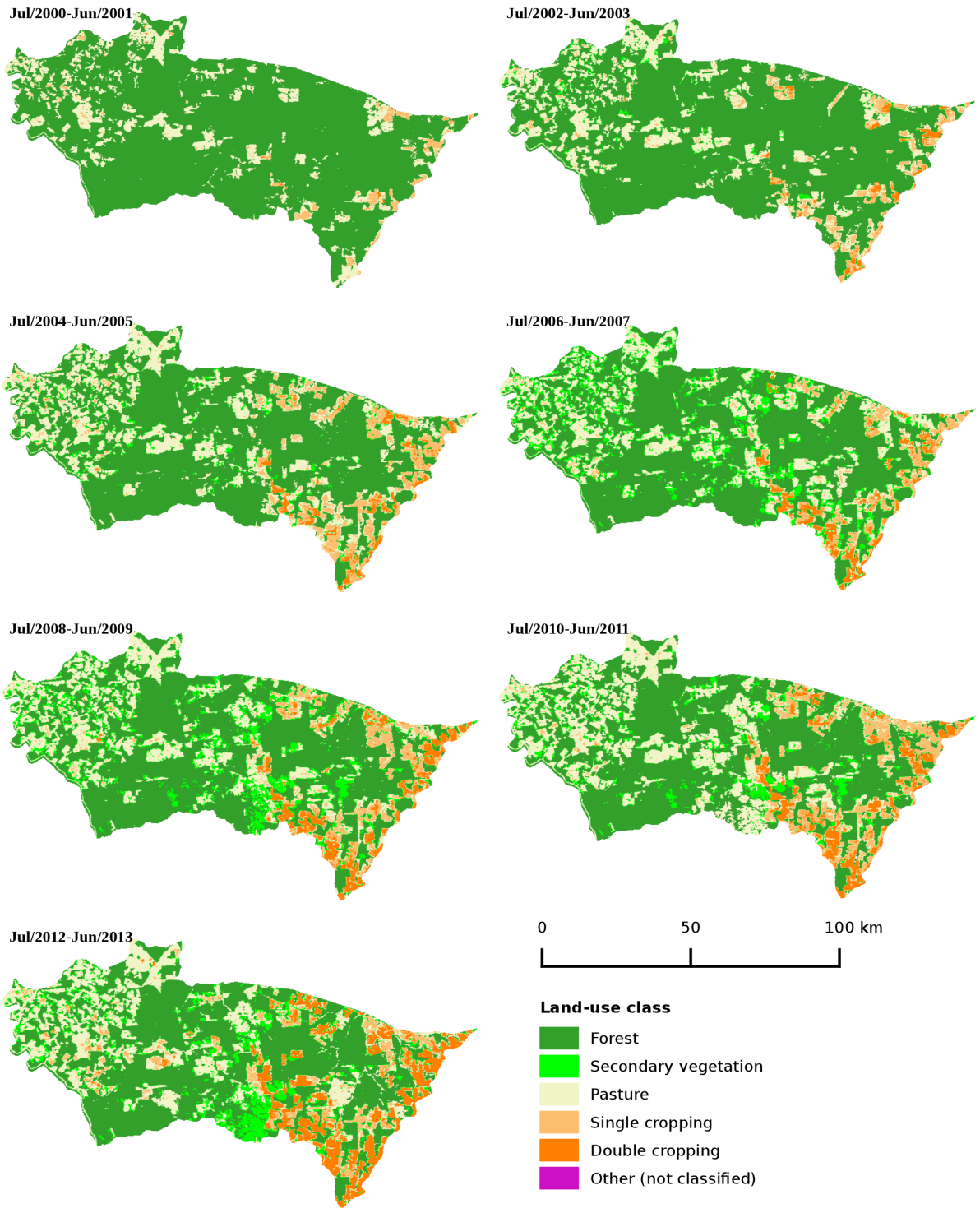

Fig. 10: Land use/cover maps produced by using the logistic TWDTW classification. Each map shows the classification for an agricultural year (from July to June) in Porto dos Gaúchos.

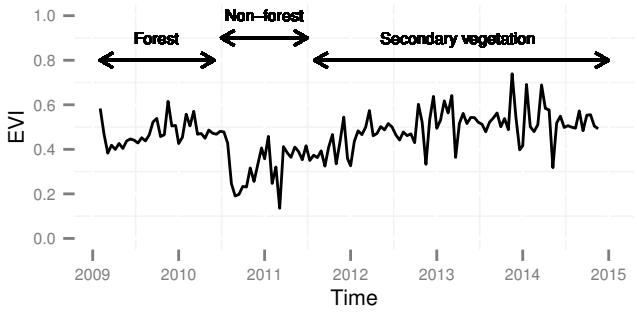

Fig. 11: An example of a classification using the transition rules. This is a sample time series inside of a burned area. This area was degraded in 2011 according to the Detection of Forest Degradation Program (DEGRAD) [39].

from the forest area only the deforestation by clear-cutting, i.e. it reduces the forest area only when most or all the trees are uniformly removed.

VI. Conclusion

In this paper we propose a Time-Weighted Dynamic Time Warping algorithm based method for land use and land cover classification of remote sensing time series. The method is a variation of the well-known dynamic time warping (DTW) method for data mining in time series. DTW works with a small amount of patterns training samples. We extended DTW to include a temporal restriction that accounts for the inter-annual variability of land cover classes. In the paper, we show that the method achieves a high accuracy for mapping classes of single cropping, double cropping, forest, and pasture in a tropical forest area.

We compared the proposed algorithm with alternative methods of using the dynamic time warping technique for land cover and land use mapping. Among the other tested variations of DTW, the algorithm without time restrictions had the worst results. The linear TWDTW method, that has a large time-weight, also has unsatisfactory results. The second-best result was obtained by the DTW method with a fixed time delay. The time-weighted DTW had better results than the alternatives that use DTW, and also achieved good overall results, with a global accuracy of 87.32%.

Our classification using the logistic TWDTW has higher accuracy and spatial resolution than the MODIS land cover product. Forest and cropland areas are in line with the Amazon Monitoring Program PRODES and with the Brazilian national cropland surveys, respectively. These results highlight the potential of the TWDTW to improve land use and land cover products and contribute to agricultural statistics.

Acknowledgements

Victor Maus has been supported by the Institute for Geoinformatics, University of Münster (Germany), and by the Earth System Science Center, National Institute for Space Research (Brazil). Part of the research was developed in the Young Scientists Summer Program at the International Institute for Systems Analysis, Laxenburg (Austria). Gilberto Camara's term as Brazil Chair at IFGI has been supported by CAPES (grant 23038.0075692012-16). Gilberto's work is also supported by FAPESP e-science program (grant 2014-08398-6) and CNPq (grant 3121512014-4).

References

[1] G. J. Roerink, M. Menenti, and W. Verhoef, "Reconstructing cloudfree ndvi composites using fourier analysis of time series," *International Journal of Remote Sensing*, vol. 21, no. 9, pp. 1911–1917, 2000.

[2] R. S. Lunetta, J. F. Knight, J. Ediriwickrema, J. G. Lyon, and L. D. Worthy, "Land-cover change detection using multi-temporal modis ndvi data," *Remote Sensing of Environment*, vol. 105, no. 2, pp. 142 – 154, 2006.

[3] J. Verbesselt, R. Hyndman, G. Newnham, and D. Culvenor, "Detecting trend and seasonal changes in satellite image time series," *Remote Sensing of Environment*, vol. 114, no. 1, pp. 106–115, 2010.

[4] J. Verbesselt, A. Zeileis, and M. Herold, "Near real-time disturbance detection using satellite image time series," *Remote Sensing of Environment*, vol. 123, no. 0, pp. 98 – 108, 2012.

[5] P. Jönsson and L. Eklundh, "Seasonality extraction by function fitting to time-series of satellite sensor data," *IEEE Transactions on Geoscience and Remote Sensing*, vol. 40, no. 8, pp. 1824–1832, 2002.

[6] P. Griffiths, S. van der Linden, T. Kuemmerle, and P. Hostert, "A pixel-based landsat compositing algorithm for large area land cover mapping," *Selected Topics in Applied Earth Observations and Remote Sensing, IEEE Journal of*, vol. 6, no. 5, pp. 2088–2101, Oct 2013.

[7] R. E. Kennedy, Z. Yang, and W. B. Cohen, "Detecting trends in forest disturbance and recovery using yearly landsat time series: 1. landtrendr – temporal segmentation algorithms," *Remote Sensing of Environment*, vol. 114, no. 12, pp. 2897–2910, 2010.

[8] Z. Zhu, C. E. Woodcock, and P. Olofsson, "Continuous monitoring of forest disturbance using all available landsat imagery," *Remote Sensing of Environment*, vol. 122, no. 0, pp. 75–91, 2012, landsat Legacy Special Issue.

[9] B. DeVries, J. Verbesselt, L. Kooistra, and M. Herold, "Robust monitoring of small-scale forest disturbances in a tropical montane forest using landsat time series," *Remote Sensing of Environment*, vol. 161, no. 0, pp. 107 – 121, 2015.

[10] X. Xiao, S. Boles, J. Liu, D. Zhuang, S. Frolking, C. Li, W. Salas, and B. M. III, "Mapping paddy rice agriculture in southern china using multi-temporal MODIS images," *Remote Sensing of Environment*, vol. 95, no. 4, pp. 480 – 492, 2005.

[11] B. D. Wardlow, S. L. Egbert, and J. H. Kastens, "Analysis of time-series MODIS 250m vegetation index data for crop classification in the u.s. central great plains," *Remote Sensing of Environment*, vol. 108, no. 3, pp. 290 – 310, 2007.

[12] F. Petitjean, J. Inglada, and P. Gancarski, "Satellite image time series analysis under time warping," *Geoscience and Remote Sensing, IEEE Transactions on*, vol. 50, no. 8, pp. 3081–3095, 2012.

[13] G. le Maire, S. Dupuy, Y. Nouvellon, R. A. Loos, and R. Hakamada, "Mapping short-rotation plantations at regional scale using MODIS time series: Case of eucalypt plantations in brazil," *Remote Sensing of Environment*, vol. 152, no. 0, pp. 136 – 149, 2014.

[14] G. L. Galford, J. F. Mustard, J. Melillo, A. Gendrin, C. C. Cerri, and C. E. Cerri, "Wavelet analysis of MODIS time series to detect expansion and intensification of row-crop agriculture in brazil," *Remote Sensing of Environment*, vol. 112, no. 2, pp. 576–587, 2008.

[15] T. Sakamoto, P. C. Van, Kotera, K. D. Nguyen, and M. Yokozawa, "Analysis of rapid expansion of inland aquaculture and triple rice-cropping areas in a coastal area of the vietnamese mekong delta using MODIS time-series imagery," *Landscape and Urban Planning*, vol. 92, no. 1, pp. 34–46, 2009.

[16] V. Velichko and N. Zagoruyko, "Automatic recognition of 200 words," *International Journal of Man-Machine Studies*, vol. 2, no. 3, pp. 223–234, 1970.

[17] H. Sakoe and S. Chiba, "A dynamic programming approach to continuous speech recognition," in *Proceedings of the Seventh International Congress on Acoustics, Budapest*, vol. 3. Budapest: Akadémiai Kiadó, 1971, pp. 65–69.

[18] ——, "Dynamic programming algorithm optimization for spoken word recognition," *Acoustics, Speech and Signal Processing, IEEE Transactions on*, vol. 26, no. 1, pp. 43–49, feb 1978.

[19] L. Rabiner and B.-H. Juang, *Fundamentals of speech recognition*. Prentice-Hall International, Inc., 1993.

[20] D. J. Berndt and J. Clifford, "Using dynamic time warping to find patterns in time series." in *KDD Workshop*, U. M. Fayyad and R. Uthurusamy, Eds. AAAI Press, 1994, pp. 359–370.

[21] E. Keogh and C. A. Ratanamahatana, "Exact indexing of dynamic time warping," *Knowledge Information Systems*, vol. 7, no. 3, pp. 358–386, 2005.

[22] Y.-S. Jeong, M. K. Jeong, and O. A. Omitaomu, "Weighted dynamic time warping for time series classification," *Pattern Recognition*, vol. 44, no. 9, pp. 2231 – 2240, 2011, computer Analysis of Images and Patterns.

[23] B. C. Reed, J. F. Brown, D. VanderZee, T. R. Loveland, J. W. Merchant, and D. O. Ohlen, "Measuring phenological variability from satellite imagery," *Journal of Vegetation Science*, vol. 5, no. 5, pp. 703–714, 1994.

[24] X. Zhang, M. A. Friedl, C. B. Schaaf, A. H. Strahler, J. C. Hodges, F. Gao, B. C. Reed, and A. Huete, "Monitoring vegetation phenology using MODIS," *Remote Sensing of Environment*, vol. 84, no. 3, pp. 471 – 475, 2003.

[25] F. Petitjean and J. Weber, "Efficient satellite image time series analysis under time warping," *Geoscience and Remote Sensing Letters, IEEE*, vol. 11, no. 6, pp. 1143–1147, June 2014.

[26] M. Müller, *Information Retrieval for Music and Motion*. London: Springer, 2007.

[27] A. Huete, H. Liu, K. Batchily, and W. van Leeuwen, "A comparison of vegetation indices over a global set of TM images for EOS-MODIS," *Remote Sensing of Environment*, vol. 59, no. 3, pp. 440–451, 1997.

[28] A. Huete, K. Didan, T. Miura, E. Rodriguez, X. Gao, and L. Ferreira, "Overview of the radiometric and biophysical performance of the MODIS vegetation indices," *Remote Sensing of Environment*, vol. 83, no. 1-2, pp. 195–213, 2002.

[29] R. M. de Freitas, E. Arai, M. Adami, A. S. Ferreira, F. Y. Sato, Y. E. Shimabukuro, R. R. Rosa, L. O. Anderson, and B. F. T. Rudorff, "Virtual laboratory of remote sensing time series: visualization of MODIS EVI2 data set over south america," *Journal of Computational Interdisciplinary Sciences*, vol. 2, no. 1, pp. 57–68, 2011.

[30] S. Mallat, *A Wavelet Tour of Signal Processing*, 2nd ed. San Diego, California, USA: Academic Press An imprint of Elsevier, 1998.

[31] T. Sakamoto, M. Yokozawa, H. Toritani, M. Shibayama, N. Ishitsuka, and H. Ohno, "A crop phenology detection method using time-series MODIS data," *Remote Sensing of Environment*, vol. 96, no. 3-4, pp. 366–374, 2005.

[32] INPE (National Institute for Space Research, Brazil). (2014) Amazon Deforestation Monitoring Project - PRODES. [Online]. Available: www.obt.inpe.br/prodes

[33] A. P. D. Aguiar, G. Câmara, and M. I. S. Escada, "Spatial statistical analysis of land-use determinants in the Brazilian Amazonia: Exploring intra-regional heterogeneity," *Ecological Modelling*, vol. 209, no. 24, pp. 169 – 188, 2007.

[34] INPE (National Institute for Space Research, Brazil). (2008) Amazon land use database - TerraClass. [Online]. Available: www.inpe.br/cra/projetos_pesquisas/terraclass2008/

[35] IBGE (Brazilian Institute of Geography and Statistics). (2014) Municipal Agricultural Production - PAM. [Online]. Available: www.sidra.ibge.gov.br/bda/

[36] D. Arvor, M. Jonathan, M. S. o. P. Meirelles, V. Dubreuil, and L. Durieux, "Classification of MODIS EVI time series for crop mapping in the state of mato grosso, brazil," *International Journal of Remote Sensing*, vol. 32, no. 22, pp. 7847–7871, 2011.

[37] Google Earth Engine. (2014) Google Earth Engine. [Online]. Available: https://earthengine.google.org/

[38] M. A. Friedl, D. Sulla-Menashe, B. Tan, A. Schneider, N. Ramankutty, A. Sibley, and X. Huang, "Modis collection 5 global land cover: Algorithm refinements and characterization of new datasets," *Remote Sensing of Environment*, vol. 114, no. 1, pp. 168 – 182, 2010.

[39] INPE (National Institute for Space Research, Brazil). (2014) Detection of forest degradation (DEGRAD). [Online]. Available: www.obt.inpe.br/degrad/